this oxygen reduction potential, in the acidic range, is about 100 mV positive of the main reduction wave, now assigned to $M^{I}[Cl_{16}Pc(-2)]^{-}/M^{I}[Cl_{16}Pc(-3)]^{2-}$, the inference is that the $M^{II}[Cl_{16}Pc(-2)]/[M^{I}[Cl_{16}Pc(-2)]^{-}$ couple is very close to and perhaps partially obscured by the main reduction processes. This adds support to the argument that the $M^{II}[Cl_{16}Pc(-2)]/[M^{I}[Cl_{16}Pc(-2)]^{-}$ process is represented by the shoulder on the positive potential side of the main reduction wave in acidic medium.

Conclusions

Perchlorination of the phthalocyanine ring leads to derivatives whose properties are clearly modified by the electron-withdrawing substituents. The species are much easier to reduce but more difficult to oxidize. The change in pH dependence for the $Fe^{III}[Cl_{16}Pc(-2)]^{+}/Fe^{II}[Cl_{16}Pc(-2)]$ couple relative to unsubstituted FePc reveals a new procedure for the tuning of a redox potential, in this case through a combination of pH control and ring substitution. In particular the central metal ion has gained additional Lewis acid character. The lack of clear observation of the $M^{II}[Cl_{16}Pc(-2)]/M^{I}[Cl_{16}Pc(-2)]^{-}$ redox process may arise through very sluggish kinetics, a consequence of the chlorine substitution generating aggregates, causing the wave to be broadened over an appreciable potential range. Further studies with other central metal ions are likely to prove rewarding.

Acknowledgment. We are indebted to the Natural Sciences and Research Council (Ottawa) and to the Office of Naval Research (Washington, DC) for financial support. We are indebted to Union Carbide, Parma, for a gift of highly oriented pyrolytic graphite.

Contribution from the Unité 219 de l'Institut National de la Santé et de la Recherche Médicale, Institut Curie, Section de Biologie, Centre Universitaire, 91405 Orsay, France

Influence of Distal Steric Hindrance on Multiple Energy Barriers in Ligand Binding to Heme Model Compounds

Catherine Tetreau,* Michel Momenteau, and Daniel Lavalette

Received June 19, 1989

The temperature dependence of carbon monoxide and oxygen binding to new "hybrid" heme model compounds has been investigated in liquid toluene between 180 and 320 K by laser flash photolysis. The heme models had been devised to present, on their distal face, a strong central steric hindrance. These compounds (except perhaps one) were found to react according to a double-barrier energy scheme, as already observed with basket-handle porphyrins. On moving along the reaction coordinate, the ligand must first overcome a free energy barrier due to the steric hindrance on the distal side. This external barrier and also the top of the internal energy barrier associated with bond formation are both increased in the more encumbered hemes. The ΔG changes are found to be nearly identical for CO and O_2, showing that steric discrimination against CO does not occur in the transition states. However, the relative contributions of enthalpy and entropy to the free energy changes associated with the innermost transition state differ sharply with the ligand.

Introduction

It is now generally recognized that binding of ligands to heme proteins is regulated by multiple free energy barriers.[1-3] Recently, we have reported that the reaction of oxygen and carbon monoxide with sterically protected heme model porphyrins, e.g. the basket-handle porphyrin **2**, (see Chart I), was similarly governed by two sequential barriers, whereas only one was found for a porphyrin devoid of any distal protection, e.g. compound **1**.[4] At a distance of 6-7 Å, the distal chain does not interfere with the Fe-O-O or Fe-C-O bond formation but produces a "matrix" effect, which is at the origin of the external barrier, by opposing the free diffusion of the ligand from the solvent. The innermost barrier remains characteristic of the ultimate bond formation process. These findings are consistent with a "peripheral" steric effect.[5,6] In an attempt to produce a strong "central" steric effect,[5,6] the "hybrid" models **3-5** have been recently synthesized.[7] Here, the pivalamido pickets are expected to maintain the "amide handle" approximately within a plane. However, since the possibility of anchoring an internal chelated proximal base is lost in **3-5**, an external nitrogenous ligand must be added to provide pentacoordination of the iron. Because of the distal steric hindrance, the base preferentially binds on the unprotected side of the porphyrin and leaves the encumbered distal cage for gaseous ligand binding. The most striking effect of increasing central steric hindrance from compound **3** to **5** is a reduction by a factor of 2500 of the affinity constant for CO while oxygen binding is reduced by less than a factor of 5 (at 293 K). Moreover, the changes affect mainly the "on" rate for CO while both "on" and "off" rates are changed in the case of oxygen.[7] Thus, constraining the handle in such a central position results in an increased sensitivity of rate and equilibrium constants upon changing the length of the distal chain.

The understanding of these effects, however, requires an investigation of the number and nature of the energy barriers. For this purpose, we investigate in this work the temperature dependence of the rate of CO and O_2 binding to 1-methylimidazole pentacoordinated porphyrins **3-5**.

Materials and Methods

The synthesis and characterization of porphyrins **3-5** as well as the procedures used for preparing the carboxy- and oxyhemochromes have been described previously.[7,8] Reduction to the Fe(II) forms was performed by using sodium dithionite in wet toluene under anaerobic conditions.[9] The pentacoordinated porphyrins were obtained by addition of a deaerated solution of 1-methylimidazole (1-MeIm). The solutions (about 5×10^{-5} M in toluene) were rendered anhydrous by prolonged bubbling with pure argon or CO. The final equilibration of the solutions

(1) Austin, R. H.; Beeson, K. W.; Eisenstein, L.; Frauenfelder, H.; Gunsalus, I. C. *Biochemistry* **1975**, *14*, 5355.
(2) Beece, D.; Eisenstein, L.; Frauenfelder, H.; Good, D.; Marden, M. C.; Reinisch, L.; Reynolds, A. H.; Sorensen, L. B.; Yue, K. T. *Biochemistry* **1980**, *19*, 5147.
(3) Ansari, A.; Di Iorio, E. E.; Dlott, D. D.; Frauenfelder, H.; Iben, I. E. T.; Langer, P.; Roder, H.; Sauke, T. B.; Shyamsunder, E. *Biochemistry* **1986**, *25*, 3139.
(4) Tetreau, C.; Lavalette, D.; Momenteau, M.; Lhoste, J. M. *Proc. Natl. Acad. Sci. U.S.A.* **1987**, *84*, 2267.
(5) Traylor, T. G.; Campbell, D.; Tsuchiya, S.; Mitchell, M.; Stynes, D. V. *J. Am. Chem. Soc.* **1980**, *102*, 5939.
(6) Hashimoto, T.; Dyer, R. L.; Crossley, M. J.; Baldwin, J. E.; Basolo, F. *J. Am. Chem. Soc.* **1982**, *104*, 2101.
(7) Momenteau, M.; Loock, B.; Tetreau, C.; Lavalette, D.; Croisy, A.; Schaeffer, C.; Huel, C.; Lhoste, J. M. *J. Chem. Soc., Perkin Trans. 2* **1987**, 249.
(8) Lavalette, D.; Tetreau, C.; Mispelter, J.; Momenteau, M.; Lhoste, J. M. *Eur. J. Biochem.* **1984**, *145*, 555.
(9) Momenteau, M. *Biochem. Biophys. Acta* **1973**, *304*, 814.

0020-1669/90/1329-1727$02.50/0

Chart I

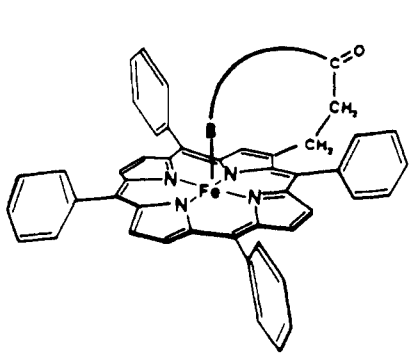

1 : B = -O-$(CH_2)_3$-

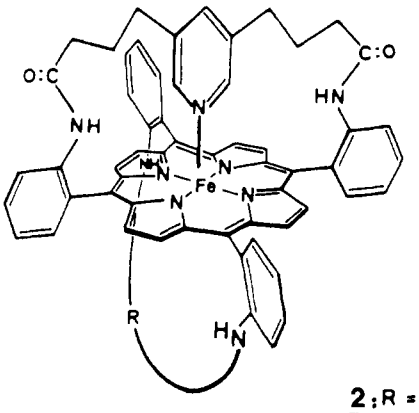

2 : R = CO-$(CH_2)_{10}$-CO

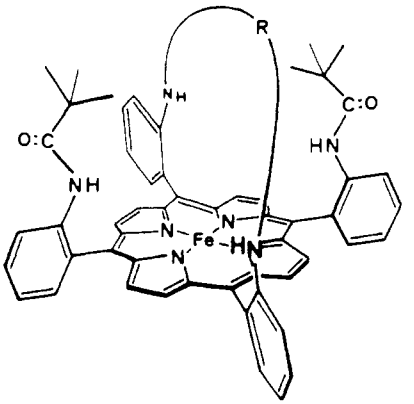

3 : R = CO-$(CH_2)_{10}$-CO

4 : R = CO-$(CH_2)_8$-CO

5 : R = CO-$(CH_2)_6$-CO

with the desired gas mixture was performed in a thermostated cell. For the solubility of oxygen and carbon monoxide in toluene at 293 K, we used the published values: 7.2×10^{-3} M·atm^{-1} (CO) and 5.3×10^{-3} M·atm^{-1} (O_2).[10] The solubilities at higher temperatures were estimated by using the results of independent kinetic measurements performed on compound **1**. At all temperatures, the pseudo-first-order rebinding rates of O_2 and CO are respectively $k_{CO} = \lambda'_{CO}[CO]$ and $k_{O_2} = \lambda'_{O_2}[O_2]$. The rebinding of CO and O_2 with **1** has been found previously to follow accurately a simple Arrhenius law in the 180–290 K interval.[4] Therefore, the true second-order rate constants λ'_{CO} and λ'_{O_2} could be extrapolated above 290 K by using the Arrhenius parameters. The concentrations [CO] and [O_2] were then deduced from additional measurements of k_{CO} and k_{O_2} performed at the desired temperature. Statistical analysis gave an estimate of ±3% for the standard deviation of the second-order rates λ'_{O_2} or λ'_{CO} extrapolated above 290 K. Individual pseudo-first-order rates are determined currently with about 5% accuracy. Therefore, the solubilities estimated in this way are accurate to within about ±10%. For measurements below 293 K, a different procedure was used: the equilibration was accomplished at 293 K, but the solution was transferred into a gastight cell that was completely filled with liquid. In the absence of a gaseous phase, practically no reequilibration could occur upon lowering the temperature, and the values of the solubilities at 293 K were simply corrected to account for the small solvent contraction. The samples were finally inserted into a thermostated cell holder (for $T > 293$ K) or an Oxford Instruments DN704 cryostat (for $T < 293$ K). In both cases the temperature was kept constant within about 0.5 K. In practice, the useful temperature range was from 180 up to 320 K. The lower limit was imposed by the requirement to keep the solution fluid and transparent. Since crystallographic data[11-13] show that no atropisomerization of free-base porphyrins **3**–**5** occurs even after 1–2 h of heating at 340 K, we arbitrarily adopted 320 K as the highest working temperature in the present study.

The association rate constants of oxygen and carbon monoxide with 1-MeIm pentacoordinated porphyrins **3**–**5** were obtained from the rebinding kinetics following photodissociation of the carboxyhemochromes and oxyhemochromes by a laser pulse using the apparatus described previously.[14] In contrast to chelated porphyrins like **1** and **2**, which exist spontaneously as pentacoordinated species, the hybrid models require an external base, which is added to the solution. If the base concentration is too low, photodissociation of the gaseous ligand may lead to base elimination. This generally results in an apparent rate of rebinding that is too fast, in particular for CO.[15] On the contrary, if the external base is present in a too large excess, photodissociation may be followed by the transient formation of a hemochrome (i.e. the hexacoordinated species containing two molecules of the nitrogenous base), and the subsequent rebinding is in fact an exchange reaction.[14] Since both processes are dependent on the base concentration, the measurements were repeated at several 1-MeIm concentrations. Except in a few cases, it has been generally possible to determine a concentration range within which the rebinding rate of O_2 and CO remained independent of base concentration. It was eventually also necessary to speed up or to slow down the overall reaction by adjusting the concentration of the gaseous ligand. In principle, the whole procedure must be repeated at each temperature since the various kinetic processes involved may present a different temperature dependence. In practice, a complete run was performed at 40 K intervals and interpolated for measurements at intermediate temperatures. The concentration of 1-MeIm varied from 10^{-4} to 2×10^{-2} M. Gas concentrations were always at least 10 times the porphyrin concentration so that the pseudo-first-order approximation could be applied throughout. Tables SI–SVI give the kinetic data, and Table SVII gives the temperature dependence of O_2 and CO solubilities (see supplementary material).

Results and Discussion

Rebinding of O_2 and CO with the hybrid porphyrins **3**–(1-MeIm) to **5**–(1-MeIm) was found to be exponential and, as expected, pseudo-first-order with respect to the concentration of the gaseous ligands over the whole temperature range. The computed

(10) Linke, W.; Seidell, A. *Solubilities of Inorganic and Metal-Organic Compounds*; Van Nostrand: Princeton, NJ, 1958.
(11) Ricard, L.; Weiss, R.; Momenteau, M. *J. Chem. Soc., Chem. Commun.* **1986**, 818.
(12) Fischer, J.; Weiss, R.; Momenteau, M. Unpublished results.
(13) Momenteau, M.; Scheidt, W. R.; Eigenbrot, C. W.; Reed, C. A. *J. Am. Chem. Soc.* **1988**, *110*, 1207.
(14) Lavalette, D.; Tetreau, C.; Momenteau, M. *J. Am. Chem. Soc.* **1979**, *101*, 5395.
(15) Cannon, J.; Geibel, J.; Whipple, M.; Traylor, T. G. *J. Am. Chem. Soc.* **1976**, *98*, 3395.

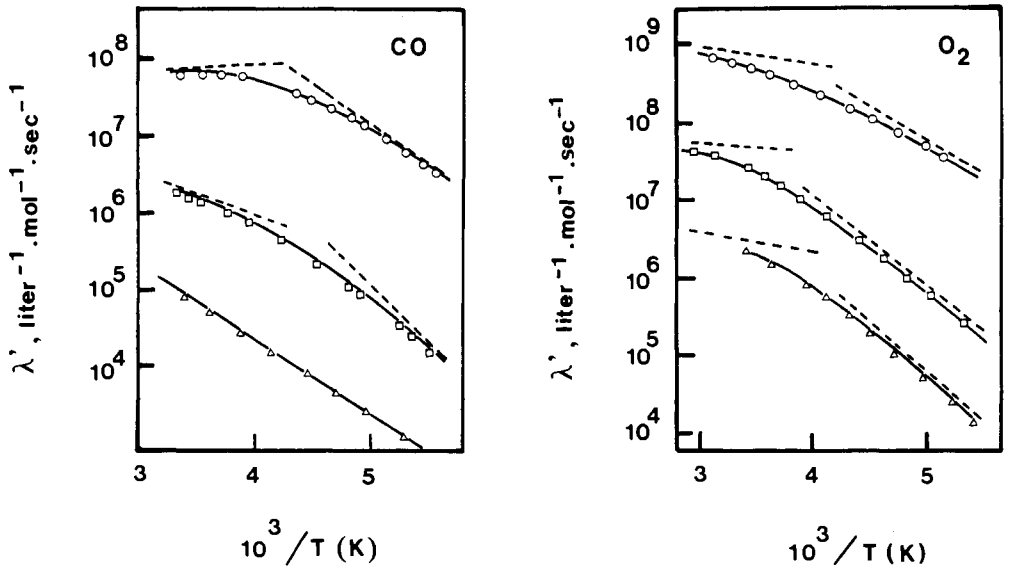

Figure 1. Temperature dependence of the second-order rate parameters for binding of CO and O_2 to "hybrid" porphyrins **3**-(1-MeIm) (○), **4**-(1-MeIm) (□), and **5**-(1-MeIm) (△) in liquid toluene. Errors are smaller than or equal to the size of the data symbols. The lines drawn through the points are least-squares fits according to eq 2. The dotted lines represent the Arrhenius laws, which would be observed if the high- (k_I) or low-temperature (k_{II}) limits were reached. In practice, these asymptotic lines must be computer-calculated by using the experimental λ′ values and eq 2. The plot relative to **5**-(1-MeIm)(CO) could be fit to a single Arrhenius law.

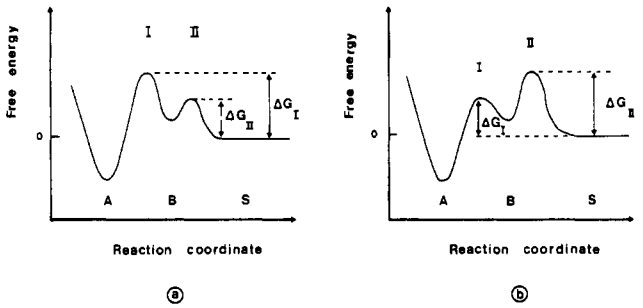

Figure 2. The double-barrier model. A is the bound state, and S, the dissociated pair (porphyrin plus ligand) in the solvent. The intermediate state B is only transiently populated. ΔG_I and ΔG_{II} refer to the top of barriers I and II relative to the reactants. In (a) the situation depicted corresponds to the high-temperature limit, in which the overall reaction rate is determined by ΔG_I. When the temperature is lowered (b), the relative height of the barriers is reversed and rebinding becomes controlled by ΔG_{II}. At about 300 K, the reaction of CO with heme models as well as with hemoproteins corresponds approximately to case a. With O_2, an intermediate situation is usually observed with $\Delta G_I \simeq \Delta G_{II}$.

second-order rate constant varied with temperature, as shown in Figure 1. Except for CO rebinding with **5**-(1-MeIm), the Arrhenius plots deviate significantly from a straight line. This result is similar to our previous findings for the association of ligands with the basket-handle porphyrin **2**.[4] It was shown that the simplest scheme which fits the data requires two transition states and two free energy barriers in sequence (Figure 2).

The relevant kinetic system is shown in Scheme I, where A is the heme–ligand bound state, S is the dissociated pair in the solvent, and B is an intermediate state that is only transiently

Scheme I

$$A \xleftarrow{k_{BA}} B \underset{k'_{SB}}{\overset{k_{BS}}{\rightleftharpoons}} S$$

populated, k_{BA} and k_{BS} are first-order rates, and k'_{SB} is a second-order rate constant. Because of the high affinity for the ligands, the dissociation rate k_{AB} is usually neglected. Immediately after the heme–ligand bond has been broken upon photodissociation, the system is assumed to be in state B. Experimentally, the rebinding kinetics show first a very fast first-order geminate recombination B → A followed by a much slower bimolecular phase, implying ligand molecules that have escaped into the solvent.[1-4] In heme model compounds, the geminate phase is in the picosecond to nanosecond time range,[16,17] which is much too fast for observation owing to the pulse width (20 ns) of our laser. In the present work, we studied the slower rebinding from the solvent, which, according to Scheme I, is described by the apparent second-order rate constant

$$\lambda' = k'_{SB}\frac{k_{BA}}{k_{BA} + k_{BS}} \quad (1)$$

This can be rewritten as

$$\lambda'^{-1} = k_I^{-1} + k_{II}^{-1} \quad (2)$$

where $k_I = k_{BA}k'_{SB}/k_{BS}$ and $k_{II} = k'_{SB}$ are limiting rates that are observed at high or low temperature when barrier I or II dominates, respectively (see Figure 2). The statement that barrier II increases faster than barrier I upon lowering the temperature is based on the observation that the fraction of ligands which escape into the solvent is always found to decrease at low temperature.[4] Each of the limiting rates k_I and k_{II} follows independently an apparent Arrhenius law corresponding to the linear asymptotic parts of the curved plots of Figure 1. Using this model, a computer fit of the data (full lines in Figure 1) yields the activation energy

Table I. Calculated Apparent Arrhenius Parameters of the Limiting Rates k_I and k_{II} (Eq 1) for Binding of O_2 and CO to Sterically Encumbered Heme Models **3**–**5**

model	ligand	E_I, kJ·mol⁻¹	log A_I	E_{II}, kJ·mol⁻¹	log A_{II}
3-(1-MeIm)	O_2	4.6	9.8	17.6	12.3
	CO	−1.4	7.6	20.2	12.4
4-(1-MeIm)	O_2	3.1	8.3	23.7	11.9
	CO	11.0	8.2	27.6	12.3
5-(1-MeIm)	O_2	4.5	7.3	26.8	11.6
	CO	18.8	8.3		
mean error[a]	O_2	±3.5	±0.6	±1.6	±0.5
	CO	±1.0	±0.2	±0.4	±0.9

[a] Errors are the averaged standard deviations of the estimates of the least-squares fits. They are higher for O_2 than for CO because the high- or low-temperature limits described by the asymptotic lines could not be reached in the investigated T range.

(16) Alberding, N.; Austin, R. H.; Chan, S. S.; Eisenstein, L.; Frauenfelder, H.; Gunsalus, I. C.; Nordlund, T. M. *J. Chem. Phys.* **1976**, *65*, 4701.
(17) Caldwell, K.; Noe, L. J.; Ciccone, J. D.; Traylor, T. G. *J. Am. Chem. Soc.* **1986**, *108*, 6150.

Table II. Overall Rate Parameters and Calculated Free Energy Variations at 293 K According to the Free Energy Diagram of Figure 1, for Binding of O_2 and CO to Porphyrins **3**–(1-MeIm) to **5**–(1-MeIm)

model		k_{on},[a] $M^{-1}\cdot s^{-1}$	k_{off},[a] s^{-1}	K_{eq},[a] M^{-1}	ΔG_{eq},[b] kJ·mol^{-1}	ΔG_I,[c] kJ·mol^{-1}	ΔG_{II},[c] kJ·mol^{-1}
3–(1-MeIm)	O_2	6.2×10^8	1.3×10^2	4.7×10^6	−37.4	21.4	20.1
	CO	6.3×10^7	2.6×10^{-3}	2.4×10^{10}	−58.1	27.6	22.1
4–(1-MeIm)	O_2	3×10^7	27	1.1×10^6	−33.8	28.3	28.4
	CO	1.8×10^6	2×10^{-3}	9×10^8	−50.1	36.5	30.4
5–(1-MeIm)	O_2	2×10^6	2	1×10^6	−34.4	35.2	33.4
	CO	8×10^4	8×10^{-3}	1×10^7	−39.2	44.0	
mean errors						±0.3	±0.9
						±0.3	±1.4

[a] From ref 7. [b] Calculated from the K_{eq} values of ref 7. [c] This work.

and the preexponential factor for the transition states I and II (Table I). In the absence of observable geminate recombination, there is no way to determine the energy of well B. It is therefore important to realize that *the E and A parameters refer to the top of each barrier measured relative to the reactants*, i.e., to the "S" state (Figure 2). Note also that k_I is a composite constant, a fact that allows for possible negative E_I values.

The relative height of both barriers depends on temperature. At high or low temperature, the asymptotic parts of the Arrhenius plots (k_I and k_{II}) can be reached, and the reactivity is almost completely controlled by barrier I or II, respectively. Situations can be encountered where one barrier always remains negligible compared to the other in the whole temperature range under investigation. This could possibly be the case of compound **5**–(1-MeIm)(CO) which showed no departure from an Arrhenius law (Figure 1). Since measurements in fluid toluene cannot be performed below −90 °C, the alternative possibility of one single energy barrier with this compound, although improbable, cannot be ruled out. From the absolute reaction rate formula and the data of Table I, the free energy changes ΔG_I and ΔG_{II} at transition states I and II were calculated. These are given in Table II together with the equilibrium values in the bound state.

Relating thermodynamic parameters and molecular structure is never unambiguous and implies that precise structural information is available. Thus, carbon monoxide has been shown to bind in a linear fashion with (*meso*-tetraphenylporphyrinato)-iron(II).[18] A linear Fe–C–O bond has been found recently in **3**–(1-MeIm)(CO).[11] Therefore, steric interference with the distal chain may be expected to persist in the bound state of the more crowded compounds **4** and **5**. On the contrary, no dramatic change of the affinity constant is expected for oxygen, which may adopt an unconstrained conformation because of the bent Fe–O–O bond.[19] Such speculations implicitly assume that the additional constraints introduced by the distal steric crowding are preferentially absorbed in chain–ligand interactions, leaving the porphyrin macrocycle untouched. To test this hypothesis, we have performed a preliminary analysis of the atomic coordinates of the carboxyhemochromes **3**–(1-MeIm)(CO) to **5**–(1-MeIm)(CO) and of the pentacoordinated species **5**–(1-MeIm), which have been recently determined by X-ray diffraction.[11-13] Contrary to expectation, we find in all CO complexes that the Fe–CO bond remains linear (within 2°) and perpendicular (within 0.5°) to the main porphyrin plane. Although the iron atom is not significantly displaced with respect to the mean plane of the porphyrinato nitrogens, the pyrrole rings exhibit a distinct ruffling distortion. The average angle of the pyrroles to the mean porphyrin plane increases continuously as the length of the chain decreases and reaches with **5**–(1-MeIm)(CO) the considerable value of 14°, which is even larger than in the corresponding pentacoordinated species (6°). In addition the meso C atoms to which the handle is anchored are displaced away from the nitrogen plane in the distal direction. As a result, the distance of the two central C atoms of the handle from the iron is increased from about 4.8 Å in the pentacoordinated species **5** to 6.9 Å in its carboxyhemochrome. This shows that the consequence of the presence of a short bridging chain is mainly a distortion of the porphyrin core instead of a bending of the iron–ligand bond. The ruffling even increases upon binding of carbon monoxide in order to accommodate the ligand in the usual linear conformation. These structural features must be kept in mind in attempting to understand the variations of the energy barriers.

External Barrier II. The outermost barrier of basket-handle porphyrins showed no clear dependence on the nature of the ligand and has been attributed to a "matrix" effect due to the presence of the distal chain, which opposes the free diffusion from the outside.[4] It was characterized by a relatively large activation energy (17–25 kJ·mol^{-1}). The activation entropy was positive, suggesting that many degrees of freedom were involved (e.g. internal rotations). Table I shows that similar trends are observed with **3**–(1-MeIm), which is the least constrained compound of the series. However, with **4** and **5** one would expect the shorter handles to present a more "rigid" hindrance. Indeed, the increase in activation energy is significant for both ligands. The variations of log A are less clear, but the data point to a slight, but regular, decrease of the positive activation entropy. The ^{1}H NMR spectra[7] indeed indicate a progressive reduction of the amplitude of the lateral movements of the handle from compound **3** to **5**. Since entropy and enthalpy contribute with an opposite sign to $\Delta G = \Delta H - T\Delta S$, the smaller the positive activation entropy, the less the compensation to ΔH. Therefore, both enthalpy and entropy terms contribute to the progressive destabilization of transition state II from compound **3** to **5** (Table I).

Transition State at Barrier I. Once within the distal cage, the ligand has to overcome the energy barrier associated with the bond formation step. As pointed out, ΔG_I is not the free energy of activation for process B → A, but represents the free energy of transition state I relative to the reactants, S (Figure 2). The parameters of the Arrhenius plots show that, for the hybrid model **3**, ΔG_I is mainly entropic (Table I). Similar to the case of basket-handle porphyrins,[4] the activation enthalpy does not significantly contribute to the inner barrier in compound **3**, suggesting that the distal chain does not interfere with bond formation. The handle is confined in a more central position because of the presence of the two pickets,[11] but it apparently remains at a distance sufficient to avoid direct steric interaction with carbon monoxide, without requiring additional distortion of the porphyrin. For the kind of reactions considered here, it has been estimated that the loss of translational and rotational degrees of freedom of the smaller reactant (O_2 or CO) might account for most of the entropy change.[20] The relative larger entropy loss of CO compared to O_2 (Table I) may thus be tentatively interpreted as reflecting the higher orientational degeneracy of the oxygenated complex as compared to the CO adduct. These observations are parallel to those previously reported for basket-handle porphyrins. The order of magnitude of the activation entropy suggests that orientational constraints and the corresponding losses of degrees of freedom of the small ligand (O_2 or CO) are important factors governing bond formation.

For the more constrained models **4** and **5**, the destabilization of transition state I of both ligands in compounds **4** and **5** points

(18) Peng, S.; Ibers, J. A. *J. Am. Chem. Soc.* **1976**, *98*, 8032.
(19) Jameson, G. B.; Rodley, G. A.; Robinson, W. T.; Gagne, R. R.; Reed, C. A.; Collman, J. P. *Inorg. Chem.* **1978**, *17*, 850.
(20) Page, M. I.; Jencks, W. P. *Proc. Natl. Acad. Sci. U.S.A.* **1971**, *68*, 1678.

to a direct interference of the handle upon the bond formation step when the chain is located at a short distance from the iron atom. In spite of similar ΔG_1 values, Table I shows that the activation energy remains close to 4 kJ·mol^{-1} for O_2 whereas it is increased by nearly 20 kJ·mol^{-1} for CO with **5**. On the contrary, A changes by more than 2 orders of magnitude for O_2, but exhibits little variation for CO along the **3–5** series. Accordingly, the origin of the destabilization of transition state I is almost purely entropic for oxygen and predominantly enthalpic for carbon monoxide. This can be understood by considering the structural modifications that must take place during the binding process. A linear orientation of carbon monoxide should be accompanied at first by an increased interaction of this ligand with the chain. At the same time the porphyrin becomes more ruffled, leaving the chain farther away from the iron in order to accommodate CO linearly. Presumably, the shorter the handle length, the more pronounced the increase of distortion required in the binding process. Using the crystallographic data relative to the penta- and hexacoordinated complexes of **5**, we calculated that the distance of the two central C atoms from the iron is increased from about 4.8 to 6.9 Å and that the ruffling distortion increases from 6 to 14° during the binding process. The energy that must be expended appears as a larger activation enthalpy in compounds **4** and **5** as compared to **3**. Binding oxygen, on the contrary, implies a bent conformation. Although crystallographic data for the O_2 complexes are not available, it does not seem necessary to assume an increase of ruffling in this case since the bent orientation would tend to release the steric constraints with the chain. The invariant activation enthalpy supports this view. The destabilization appears as entropy terms. The orientational freedom of oxygen is known to be strongly limited due to H-bonding with the amide protons. However the effect has been shown to be significant only in the bound state.[8] Orientational constraint of a different nature, e.g. the avoiding of transient lateral interactions with the protons of the methylene groups, may play a specific role in the transition state.

Thus, in addition to confirming that hybrid models also react via two sequential energy barriers, the present results indicate that steric discrimination against CO does not occur in either transition state since both are destabilized to the same extent for CO and O_2. This is partly in agreement with the findings of Traylor et al.[21] that steric effects are seen mainly in association rates and that those are changed equally for CO and O_2. However, a previous discussion of the linear free energy relationships observed in various porphyrin series[8] has shown that this behavior is not general and can only be expected for a strong central steric hindrance. Moreover, only a detailed thermodynamic study is able to reveal that the ΔG changes, although very close for O_2 and CO, are brought about by the complex interplay of enthalpic and entropic factors, which intrinsically differ with the nature of the ligand.

Supplementary Material Available: Tables SI–SVI, listing kinetic rate constants for O_2 and CO binding with compounds **3–5** as a function of the temperature and 1-MeIm and gaseous ligand concentrations, and Table SVII, giving O_2 and CO solubilities in toluene as a function of the temperature between 343 and 193 K (6 pages). Ordering information is given on any current masthead page.

(21) Traylor, T. G.; Tsuchiya, S.; Campbell, D.; Mitchell, M.; Stynes, D.; Koga, N. *J. Am. Chem. Soc.* **1985**, *107*, 604.

Contribution from the Department of Chemistry and Biochemistry, University of Windsor, Windsor, Ontario, Canada N9B 3P4

Early/Late Heterobimetallic Complexes: Syntheses and Spectral and Structural Studies of Thiolato-Bridged Ti/Cu and V/Cu Complexes

Teresa A. Wark and Douglas W. Stephan*

Received October 3, 1989

The heterobimetallic complexes $[Cp_2Ti(\mu\text{-}SMe)_2CuPCy_3]PF_6$ (**1**), $[Cp_2Ti(\mu\text{-}SR)_2Cu(NCMe)_2]PF_6$ (R = Me (**2**), R = Et (**3**)), and $[(Cp_2Ti(\mu\text{-}SMe)_2)_2Cu]PF_6$ (**4**) have been prepared and characterized. Variable-temperature NMR studies of **1** and **2** show that the preferred orientation in solution of the methyl substituents on sulfur at low temperature is one in which they adopt a cisoid disposition. Inversion at sulfur is proposed as the mechanism that leads to the time-averaged signals at ambient temperature. The energies of the fluxional processes were found to be 77 and 80 kJ/mol for **1** and **2**, respectively. Complex **2** crystallizes in the triclinic space group $P\bar{1}$, with a = 8.038 (2) Å, b = 13.169 (3) Å, c = 11.732 (3) Å, α = 109.31 (2)°, β = 106.12 (2)°, γ = 89.29 (2)°, Z = 2, and V = 1122 (1) Å^3. The structural data are consistent with a cisoid disposition of the methyl groups on sulfur. Cyclic voltammetric studies of **1–4** show that reduction of these complexes leads to complex degradation. Electronic analogues of reduced **1** and **2** were prepared by employing V(IV). The complexes $[Cp_2V(\mu\text{-}SEt)_2CuPR_3]PF_6$ (R = Ph (**5**), R = Cy (**6**)), $[Cp_2V(\mu\text{-}SR)_2Cu(NCMe)_2]PF_6$ (R = Me (**7**), R = Et (**8**)) show EPR spectra characteristic of V(IV) complexes. For complexes **5** and **6**, hyperfine coupling to Cu(I) and P is discernible. Computer simulation revealed that the coupling to Cu is 9.5 G and to P is 8.0 G. The implications of both the structural and spectroscopic parameters for these heterobimetallic complexes are discussed. The data are consistent with electronic communication between the metal centers. A dative interaction from the electron-rich d^{10} Cu(I) center to the d^0 Ti(IV) center is suggested.

Introduction

Interest in early/late heterobimetallics[1] has arisen for several reasons. The pairing of the oxophilicity of the early metals and catalytic properties of the later metals seems to be, intuitively, the combination required for carbon oxide reduction chemistry. This view is supported by observations made for heterogeneous catalysts in which late metals are dispersed on early metal supports. In these cases, the reactivity of the dispersed metal is dramatically perturbed from that of the same metal dispersed on an inert support. This phenomenon has been termed strong metal–support interaction.[2] The nature of the interactions between the support and the late metal is not clear, but a number of possibilities have been offered. These include direct metal–metal electronic communication with participation of a reduced support in the chemistry at the surface or, alternatively, cooperative activation of the substrate by the early and late metal centers.

(1) Recent examples of early/late heterobimetallic systems have been cited in ref 3–12 and reviewed in: Stephan, D. W. *Coord. Chem. Rev.* **1989**, *95*, 41.

(2) Baker, R. T. K., Tauster, S. J., Dumesic, J. A., Eds. *Strong Metal-Support Interactions*; American Chemical Society: Washington, DC, 1986.

0020-1669/90/1329-1731$02.50/0